Available online at www.sciencedirect.com
SCIENCE DIRECT®
Journal of Chromatography A, 1073 (2005) 53–61
JOURNAL OF CHROMATOGRAPHY A
www.elsevier.com/locate/chroma

Influence of the packing heterogeneity on the performance of liquid chromatography supports

J. Billen*, P. Gzil, N. Vervoort, G.V. Baron, G. Desmet

Department of Chemical Engineering, Vrije Universiteit Brussel, Pleinlaan 2, 1050 Brussels, Belgium

Available online 5 November 2004

Abstract

We report on a series of plate height and flow resistance data obtained via computational fluid dynamics simulations in a simplified two-dimensional (2D) mimic of real packed bed and monolithic columns. By varying the external porosity ($0.4 < \varepsilon < 0.8$) and the degree of packing randomness, a good qualitative insight in the relationship between the packing porosity and heterogeneity and the general chromatographic performance parameters is obtained, unbiased by any differences in phase retention factor k', mobile phase diffusivity or viscosity or intra-skeleton porosity. The results provide a quantitative support for the use of domain size reduced plate heights as a means to compare the performance of chromatographic beds with a different porosity, as it was found that packings with a similar degree of packing heterogeneity yield very similar domain size reduced h_{min}-values, nearly completely independent of the porosity. The study also clearly shows that the presence of preferential flow paths (inevitably accompanied by the presence of more clustered regions) leads to a decrease of the flow resistance, but also leads to a strong increase of the band broadening if supports with the same porosity ε and the same radial width are compared. For the presently considered 2D system, the flow resistance reduction is too small to overcome the corresponding strong increase in band broadening, such that the presence of preferential flow paths always leads to an overall increase of the separation impedance.

Keywords: Packing heterogeneity; Band broadening; Flow resistance; Computational fluid dynamics

1. Introduction

With the emerging possibilities from the currently booming monolithic column field [1–9] to produce chromatographic supports with a broad range of porosities, it would be interesting to have some general rule describing how the chromatographic properties (band broadening and flow resistance) can be expected to vary with the porosity. For the flow resistance, the relation with the bed porosity is to a certain extent described by Kozeny–Carman's law, but this law certainly does not represent all geometrical subtleties and is only valid over a small range of porosities (as is, for example, demonstrated in [10]). For the band broadening, it can be assumed on pure physical grounds that if two systems with the same particle or skeleton size would be compared, the system with the largest porosity will produce the largest plate heights, as a consequence of its larger total mass transfer distance [11]. How large exactly the difference between two systems with the same degree of packing heterogeneity can be expected to be is, however, not known. It is nearly impossible to determine this difference via an experimental route, because if one is to compare two chromatographic systems with a different porosity, they very likely will have a different degree of heterogeneity, such that the difference in band broadening will be influenced by two factors: the porosity and the packing heterogeneity.

Decoupling both effects would be very useful. If one would know what the individual contributions stemming from the porosity and the heterogeneity are, it would be possible to compare for example two different monolith production methods (or even different production batches) and to make a statement on the homogeneity of the produced skeletons, even if the monoliths have a different porosity. The possibility to decouple porosity and packing heterogeneity effects would also allow a more accurate comparison of the homogeneity

* Corresponding author. Tel.: +32 2 629 36 17; fax: +32 2 629 32 48.
E-mail address: jbillen@vub.ac.be (J. Billen).

0021-9673/$ – see front matter © 2004 Elsevier B.V. All rights reserved.
doi:10.1016/j.chroma.2004.10.042

of different packed bed columns. Especially in the case of narrow-bore columns, there seems to be a strong variation of the obtained plate heights and the bed porosity [12,13], and the link between both parameters is most certainly masked by differences in packing heterogeneity. A similar problem seems to arise if columns are packed with particles with a broad particle size distribution.

The basic work on the relation between the packing geometry and the overall band broadening is certainly that of Giddings [14]. For the description of the axial dispersion or eddy diffusion in heterogeneous packed beds [15], he introduced the concept of the coupling distances, going from the small scale trans-channel and -particle coupling distances towards the more large scale short-range interchannel and long-range interchannel coupling distances [16]. For the comparison of systems with a different geometrical scale, he introduced the concept of the reduced plate heights [17], relying on the normalization of the plate heights with a suitable geometrical scaling factor (particle size in the case of a packed bed). As advocated by Giddings [14] and Knox and coworkers [17,18], the advantage of representing the plate heights in a reduced form is that packed beds operated with different solvents (but yielding the same k') and filled with a geometrically similar packing (i.e., differing only by its geometrical scale) should yield perfectly overlapping (h, ν) curves. If they fail to do so, this can be regarded as a sign that the two columns have a different packing geometry.

In the present study, computational fluid dynamics (CFD) simulations are used to gain a general insight in how the packing porosity and the packing heterogeneity influence the plate height of chromatographic systems and how these two effects can best be isolated from each other. All calculations were carried out on artificial two-dimensional (2D) column models. These models are arrays of 2D particles. These particles can be considered to represent the particles in packed beds, but can also be considered to represent the skeleton branches in monolithic structures and the pillars in photolithographic etched columns. The particles have a freely adjustable internal porosity and molecular diffusivity, allowing the conditions to be selected such that the retention factor ($k' = 1.25$), and the mobile and stationary phase diffusion coefficients were kept constant for all considered porosities. These conditions allow isolating the effects of packing randomness and external bed porosity from any of the other experimental conditions, something which is nearly impossible to realize in real columns.

2. Considered geometries and numerical methods

In the present study, three different porosities ($\varepsilon = 0.4$, 0.6 and 0.8) were combined with three different degrees of packing heterogeneity: (i) a perfectly ordered and maximally isotropic equilateral triangular staggering (Fig. 1a); (ii) a packing with a purely short-scale randomness obtained by starting from the arrangement in Fig. 1a and by subjecting the center point of each individual particle to a random dislocation and to a random change in particle diameter; and (iii) a combined short-scale and larger scale randomness obtained by regrouping some of the particles in Fig. 1b in more tightly grouped seven-particle clusters, displacing the particles such that the shortest distance between the central particle of the cluster and each of its six neighbours is equal to 50% of the pore size of the ordered case. The random displacement distances for each individual particle were generated using the evenly distributed random number generator of MS Excel. The maximal shift of the particle centres was always equal to 90% of the pore size. The maximal variation of the particle size was always taken as 10% of the mean particle size. By scaling the distance over which the individual particles were randomly displaced to the total pore-neck diameter, it has been ensured that the degree of column heterogeneity only varies minimally between the three different porosity cases. If the random displacement distance would instead have been taken proportional to the particle size, the small porosity system would automatically have had a much more constricted pore space than the large porosity system, thus being much more heterogeneous than the large porosity case, a situation which does not correspond to ones' intuitive idea of a similar degree of heterogeneity.

The main difference between the cases in Fig. 1b and c is that in the latter clusters are formed whereas in the former the random displacement to which the position of each individual cylinder is subjected is independent of that of the neighbouring particles. In the short-scale randomness case, the velocity can hence vary from pore to pore, as the width of each pore is independent of that of its preceding or proceeding pores. In the clustered packings, on the other hand, several regions exist where a given pore width is maintained over several particle distances, such that a given fluid velocity can persist over a relatively large axial distance. In other words, differences in flow velocity persist over longer distances in the clustered packings in Fig. 1c than in the short-scale randomness cases in Fig. 1b.

It should be noted that, in order to be able to represent a sufficient microscopic detail, the geometries depicted in Fig. 1 only constitute a part of the total considered flow domain. In reality, all flow domains consisted of 126 particles and were 6 particles wide by 11 particles long, i.e., roughly twice as long than the domains represented in Fig. 1. A number of control simulations were also performed on uniform packing domains, which were geometrically scaled down by a factor of 5.

Also indicated in Fig. 1 is the definition of the domain size. Since the uniform packing geometries are completely determined by the particle diameter and by side length of the equilateral triangle forming the unit cell for the particle centre position grid, this side length emerges as the natural measure for the domain size. As it is equal to the sum of the particle (or skeleton) diameter and the pore-neck diameter, this measure also corresponds exactly to the domain sizes, which are estimated from scanning electron microscopy (SEM) pictures,

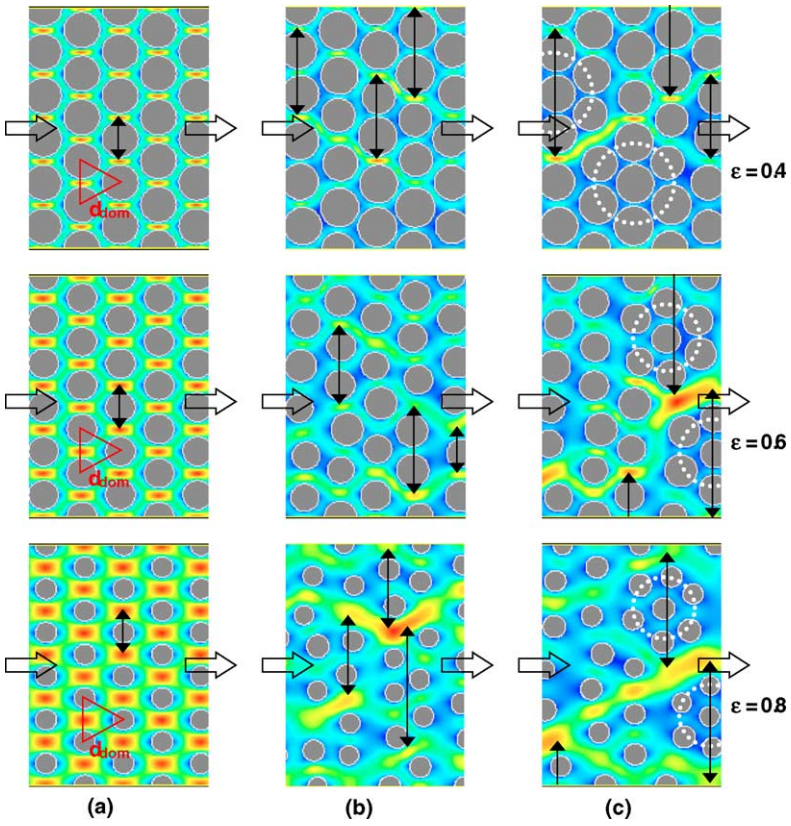

Fig. 1. Different considered 2D packing geometries (constant domain size case) and calculated velocity magnitude fields for three different porosities ($\varepsilon = 0.40$, 0.60 and 0.80), and for three different degrees of pore heterogeneity: (a) perfectly ordered equilateral triangular staggering of uniform cylinders; and a disordered packing of cylinders ((b) short-scale randomness only and (c) with mimicked cluster formation). The arrowed lines indicate the radial distance between two neighbouring preferential flow paths. The dashed circles in (c) have been added to emphasize the presence of the clusters. Details on the colour scale are given in the text. The equilateral triangle defining the grid upon which the particle center points are positioned is shown in red. The side length of this triangle determines the domain size.

where one also intuitively takes the pore-neck width and the skeleton width as the two building blocks of the domain size.

It should be noted that, unlike in a three-dimensional (3D) packed bed, the 2D particles in the 2D geometries are not allowed to touch. However, the spherical particles in a 3D packed bed also only make contact at isolated points, so that each particle can to a first approximation also be considered as being surrounded by a spherical (cylindrical in 2D) pore space shell. In 2D, the $\varepsilon = 0.4$-packing leads to a pore size equal to 23% of the particle diameter. This is slightly different from the typical 25–40%-value assumed for a 3D packing, but not too dramatic. Also the pore connectivity number is different: two in 2D versus three in a 3D packed bed and three or more in a monolith [19]. These differences will certainly cause a deviation between the currently obtained plate heights and flow resistances and those who can be expected in a 3D system. However, given that the major sources of band broadening are caused by the existence of different velocity zones and by the slowness of the radial re-equilibration diffusion process, which can as well be represented in a 2D as in a 3D case, it can be assumed that these differences will only be of secondary importance and that the presently generated data will provide a good qualitative insight in the effects under study. Apart from the dramatic reduction of the required computational efforts, a very important advantage of a 2D geometry with unconnected particles is that the position of the individual particles can easily be changed without changing the porosity, and inversely, that the porosity can be changed without modifying the position of the particles.

The procedures used to calculate the band broadening and the flow resistance for the different domains are the same as in our previous publications on the subject [20,21]. Briefly, they consist of using a commercial CFD software package (Fluent v6.1.22), in-house extended with a number of self-written numerical routines to simulate the diffusion and adsorption processes of the species, which are introduced at the inlet of the simulation domain, inside the stationary phase. The adopted approach has been validated for the classical parallel plate problem, by comparing the CFD results with the known analytical solution [22]. The accuracy of the obtained results is always verified by checking the calculation grid size and time step independence of the result. In the flow domains, radial detector lines were defined with a regular interval of 10 μm, and the radially averaged species concentration was reported as a function of time responses re-

ported for each of these lines. From these response curves, the zeroth, first and second order moments were calculated using an Euler-method based numerical integration algorithm implemented in MS Excel. From these moments, the corresponding peak migration velocities and plate heights were determined. Apart from the band broadening, the performance limits of a chromatographic system are also determined by the flow resistance. As is common tradition in chromatography [13], the flow resistance is defined on the basis of the linear velocity (u_0) of the unretained species. From the slope of these lines, it is then straightforward to calculate the resulting column permeabilities (K_v) and flow resistances (ϕ_0), using:

$$K_v = \frac{u_0 \eta L}{\Delta P} \quad \text{and} \quad \phi_0 = \frac{d_{ref}^2}{K_v} \tag{1}$$

wherein d_{ref} can be any suitable characteristic dimension (in the present study, $d_{ref} = d_{dom}$) and η is the dynamic viscosity (Pa s).

3. Results and discussion

3.1. Qualitative results

The computed velocity magnitude fields depicted in Fig. 1 all refer to cases with the same mean velocity. The velocities have been normalized with respect to the largest local velocity magnitude of each different packing case. In this way, the zones with the largest velocity are marked red and yellow (roughly $u/u_{max} > 80\%$), whereas the zones with the smallest velocities are marked blue (roughly $u/u_{max} < 10\%$). This representation automatically emphasizes the preferential flow paths. Interpreting the images, it should be noted that the area of the red and yellow zones is much smaller in the random and clustered packing cases. This does not imply that the mean velocity is smaller in these cases: it simply means that the area of the zones where the velocity is close the maximal velocity is smaller. However, it should also be remarked that the u_{max}-velocity in the more heterogeneous cases is significantly larger than the u_{max}-velocity in the uniform cases. In Fig. 1a (uniform packing case), all flow-through pores clearly have the same flow-through status, i.e., they are equally permeated and the radial distance between two neighbouring high velocity zones (red or yellow) is maximally one domain length. In the short-scale randomness case (Fig. 1b), this situation is significantly changed, as there are now only a few preferential flow paths and the radial distance between two preferential flow paths on the average roughly covers two particle diameters. Passing on to the clustered packing case (Fig. 1c), it can be concluded that the preferential flow paths are better connected (i.e., persist over a longer axial distance) and transport a larger flow rate than the short-scale randomness case. Another observation is that the radial distance between two neighbouring preferential flow paths is again significantly enlarged (three particle diameters on average) over the cases in Fig. 1b. Assessing these distances, it should be remarked here that the single headed arrows starting from the side walls of the flow domains only correspond to one half of the distance to the following high velocity zone, because the side walls are treated as symmetry planes (i.e., a zero normal concentration gradient condition on the sides of the flow domain). It should finally also be remarked that all the above observations hold to a more or less equal extent for the three considered porosity cases. The major difference between the different porosity cases is that the preferential flow paths become wider and are better axially connected if going from $\varepsilon = 0.4$ to 0.8, but this can easily be explained as a consequence of the increased porosity.

Fig. 2a–c provide a clear illustration of how the band broadening increases with Giddings' coupling distances [14]. It should be noted that whereas Fig. 2 is for the $\varepsilon = 0.4$-case, qualitatively similar species dispersion images were obtained

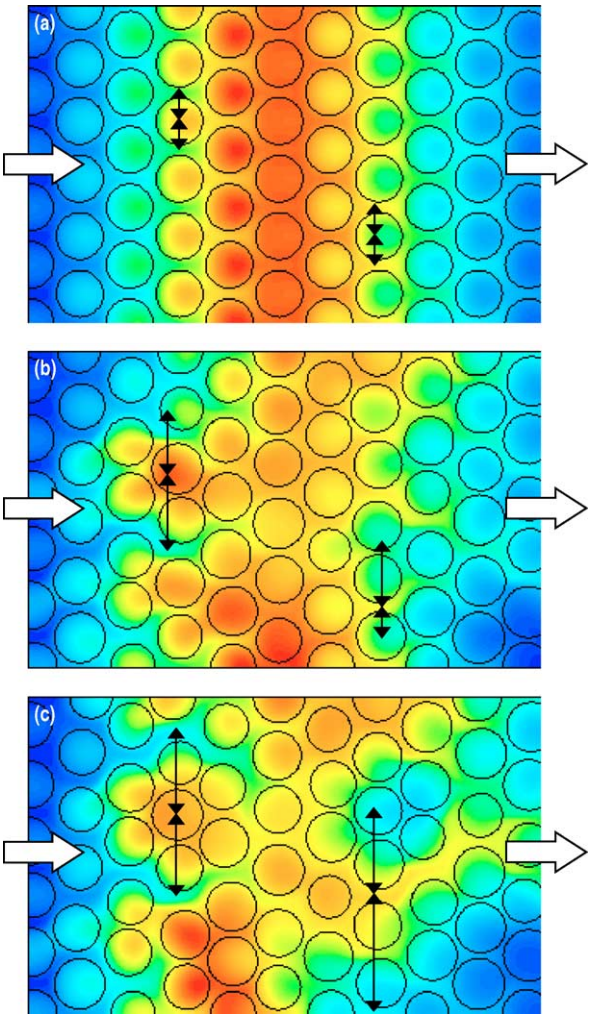

Fig. 2. Plot of species dispersion 30 ms after the introduction of the species at the inlet for a porosity of $\varepsilon = 0.4$ for the three considered degrees of packing heterogeneity: (a) homogeneous packing; (b) packing with short-scale randomness; and (c) clustered packing. The arrowed lines indicate the radial distance across which the maximal concentration difference persists.

for the other two porosities. Fig. 2a clearly shows that in the uniform packing case, the radial distance over which the maximal concentration difference persists is equal to the sum of one half of the particle diameter and one half of the pore diameter. This distance corresponds to the sum of Giddings' trans-particle and -channel coupling distances. In the short-range randomness packing cases (Fig. 2b), the band broadening is obviously much larger, as the straight band shape of the cases in Fig. 2a is completely lost. The plot clearly shows how the species in the wide pores are running ahead of those in the more densely packed regions, leading to the establishment of much longer coupling distances. Adopting Giddings' nomenclature, the maximal radial concentration difference distances denoted by the arrows in Fig. 2b could be considered as short-range coupling distances. Considering now the partially clustered packing case (Fig. 2c), it can clearly be noted that the species in the preferential flow paths surrounding the clusters run more ahead of the center of the peak than in the short-scale randomness packing in Fig. 2b. In addition, the radial distances over which the ensuing concentration differences need to be rectified are also larger, as is witnessed by the growing coupling distances. It should, however, be noted that in real columns even much longer coupling distances may be present. In the present simulation model, the largest possible coupling distance is the radial width of the flow domain. To include the effect of more long-range coupling distances it will be necessary to consider wider domains.

3.2. Quantitative results

Fig. 3 shows the calculated average plate height as a function of the reduced velocity of the unretained species for each of the nine considered geometries. Using the particle size as the reduction basis (Fig. 3a), the resulting graph is highly scattered, as the curves for the different porosities and degrees of heterogeneity are completely intertwined. Normalizing the plate height data on the basis of the domain size, on the other hand, yields a much more ordered picture (Fig. 3b). Near the minimum of the curves, the influence of the porosity is nearly completely filtered away, and the plate height curves are clearly grouped according to the three different considered degrees of heterogeneity. The h_{min}-value varies from $h_{min} \cong 0.8$ for the perfectly ordered arrays, passing over $h_{min} \cong 1.1$ for the short-scale randomness packing, and going to $h_{min} \cong 1.5$ for the clustered packings. The $\varepsilon = 0.8$ data for the clustered case slightly deviate from this value, but this is due to the fact that rules based to determine the position of the particles in the clusters are pore size related and not domain size related. Interestingly, the latter value agrees quite well with experimental values in packed bed columns, for which it is typically assumed that $H_{min} = 2d_p$ [23]. Assuming that the pore size in a packed bed is about one-third of the particle diameter, the corresponding domain size is equal to $d_{dom} = 4/3d_p$, leading to the domain size reduced $h_{min} = 1.5$-value obtained in the present

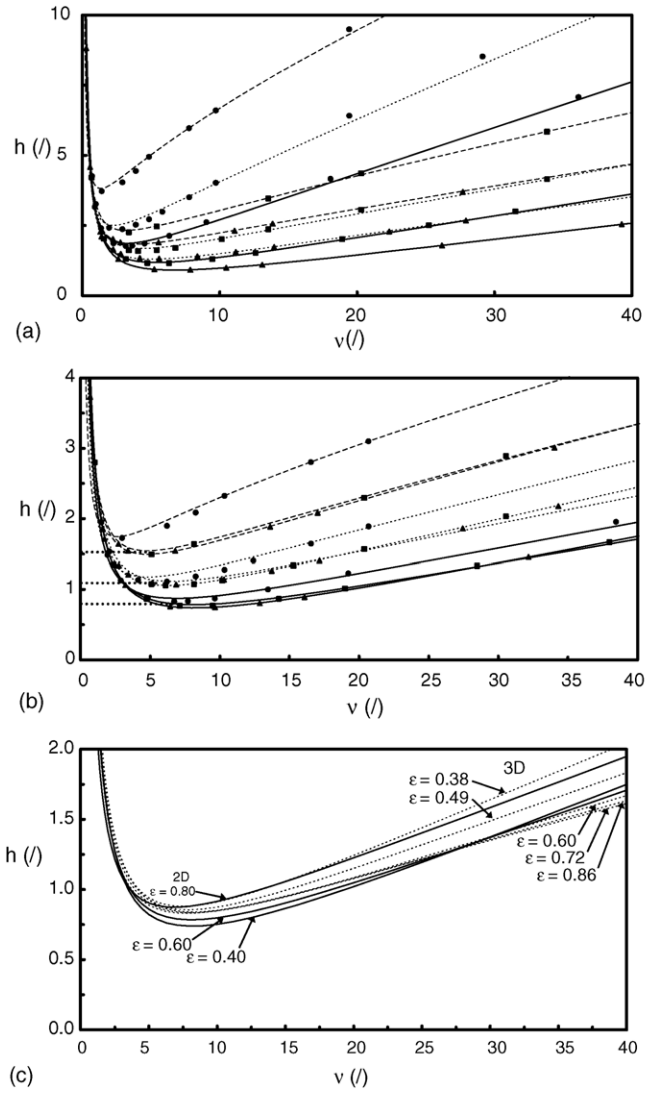

Fig. 3. Reduced Van Deemter plots of the band broadening data obtained for the three considered porosities: (▲) $\varepsilon = 0.40$; (■) $\varepsilon = 0.60$; (●) $\varepsilon = 0.80$; and a comparison with the fitted h-curves (full lines, uniform; short dashed lines, random; long dashed lines, cluster) based on the Knox equation with $n = 1/3$ (Eq. (2)). The data relate to cases with an identical phase retention factor $k' = 1.25$ and were reduced with (a) the skeleton diameter ($d_{ref} = d_s$) and (b) the domain size ($d_{ref} = d_{dom}$). In (c), the 2D uniform particle array data (full lines) are compared with the plate heights in the ordered 3D tetrahedral skeleton model (dashed lines) shown in [25] and for the same $k' = 1.25$.

study. Being packed with a silica monolith with $\varepsilon = 0.86$, the MS (50)-B and MS (50)-C columns in [7] yield a H_{min} of about 15 μm for a $d_{dom} \cong 10$ μm. This also corresponds to a value of $h_{min} \cong 1.5$. Given that we are only looking at a 2D approximation, the single prudent conclusion which can be drawn from this agreement with real packings is that the band broadening in packed beds and monolithic columns is mainly caused by the presence of clustered regions or the presence of preferential flow paths rather than by short-scale randomness effects. This is in good agreement with the generally adopted assumption that a packed bed is composed

of regions covering several particle size units with a relatively uniform, but different packing density. The same holds for monolithic columns, for which the SEMs very often reveal that a minority of the pores is significantly wider than the others. Most of the other monoliths reported in literature apparently have a much larger degree of heterogeneity than the large domain monolithic column referred to above. The MS-PTFE (B) column in [7], for example, produced a H_{min} of about 7 μm (d_{dom} = 3.85 μm, $\varepsilon \cong 0.65$), corresponding to $h_{min} \cong 1.8$. Small domain monoliths usually have even larger d_{dom}-reduced h_{min}-values, as can be noted for example from the relatively large H_{min} = 5 μm value obtained for a silica monolith with $\varepsilon \cong 0.62$ and with d_{dom} = 2.3 μm (column SR (D) in [24]). This corresponds to a value of h_{min} = 2.2. Given that it can be assumed on pure physical grounds that it is more difficult to produce small domain monoliths with the same degree of heterogeneity than large domain monoliths, this increased d_{dom}-reduced minimal plate heights can again be considered as a reflection of the increased packing heterogeneity. Maximally yielding a h_{min}-value of about 1.5, the degree of randomness in the presently considered flow domains study is apparently insufficiently strong to produce these large h_{min}-values obtained in small domain monoliths. This can either point to the fact that the displacement of the particles in the 2D model should have been subjected to a larger variance, or to the fact that the currently considered flow domains are too narrow, such that long-range coupling distance effects are excluded.

The fact that the different porosity curves do not exactly overlap, not even for the uniform packing cases (cf. the C range of the curves), points at the fact that the domain size is not able to reduce the plate height curves of different porosity systems to a single universal curve. This can be explained from the fact that the different porosity systems shown in Fig. 1a are not geometrically similar. The lack of self-similarity between the different porosity cases is a consequence of the fact that each different porosity case inevitably has a different ratio between the domain size and the particle (skeleton) size. This not only holds for the presently considered 2D arrays, but is true for all possible porous support systems (including all 3D systems). Systems with a different solid/fluid volume ratio can impossibly be overlapped one with the other by simply rescaling them, and can hence never be self-similar. On the contrary packings with the same porosity, but with a different domain or particle size, can be perfectly geometrically similar. This is also what is observed in real silica monoliths. Silica monoliths with a similar porosity usually also have pore to skeleton size ratios which are very similar, independently of the absolute value of their domain size [21]. If the porosity changes, the value of these ratios has to change, implying that two monoliths with a different porosity cannot be self-similar. The fact that self-similar geometries should yield the same domain size-reduced plate heights, as put forward by Giddings [14], has been verified by considering so-called small-domain cases for the uniform packings shown in Fig. 1a. In these small-domain cases, the dimensions of the particles were five times smaller, i.e., 2D particles with a diameter d = 1 μm were considered instead of the 5 μm in the normal domain case. The relative position of the particles was, however, left unchanged. Reducing the resulting Van Deemter curves by the particle diameter and the domain size, the obtained h-curves coincided perfectly with the uniform packing curves in, respectively, Fig. 3a and b.

Linking the obtained reduced plate height curves to the flow fields shown in Fig. 1, it can clearly be concluded that, for a given value of the external porosity, the band broadening increases with the increasing presence of preferential flow paths. When passing from Fig. 1a to c, the flow fields switch from a situation wherein all flow-through pores are equally important to a situation wherein the majority of the flow passes through a limited number of axially well-connected preferential flow paths. As each increase of the importance of the preferential flow paths is automatically accompanied by a growing size of more densely packed, hence poorly permeated zones, it can also be concluded that the larger the velocity difference between different velocity zones, the larger the axial distance over which these differences persist, and the larger the radial distance across which this velocity difference has to be wiped out, the larger the resulting band broadening can be expected to be. The notion that the band broadening in chromatographic columns can be viewed as being the result of the existence of different velocity zones connected in parallel has already been formulated long ago by Giddings [14] and others. We believe the present simulations provide a nice illustration for this viewpoint.

The fact that the different considered porosities approximately yield the same h_{min}-value implies that it should be possible to assess the degree of heterogeneity of any possible chromatographic system by simply determining the minimal plate heights for the different systems under identical k' conditions and normalizing it with respect to the domain size. Whether or not this will also hold in 3D systems obviously still needs to be verified, but it is difficult to find an argument why this would not be the case. In a sense, d_{dom}-reduced curves are currently being used on an intuitive basis in the field of silica monoliths to assess the quality of the different produced monoliths [24]. A support for the qualitative extrapolation of the present results to 3D systems is that the currently presented uniform 2D array data coincide very well with previously obtained Van Deemter curves for a 3D tetrahedral skeleton model (Fig. 3c).

Given their high accuracy, the computed CFD data are in principle also excellently suited to differentiate between the different existing plate height models. A wide variety of these models exists [16], but probably the most widespread used model is the empirical Knox n = 1/3-model [13]:

$$h = A\nu^n + \frac{B}{\nu} + C\nu, \tag{2}$$

where A, B and C are constants; h, the reduced plate height; and ν, the reduced velocity. According to Giddings' couplings theory [14], Eq. (2) should, however, better be used in its

coupled form:

$$h = \frac{1}{(1/A_e) + (1/A_m \nu)} + \frac{B}{\nu} + C\nu, \quad (3)$$

Both models were fitted to the CFD-generated data points using the standard solver function of MS Excel®. They yielded about the same quality of fitting, such that it was difficult to discriminate between them. None of both models, however, yielded a really good fit (cf. the full and dashed lines in Fig. 3b), especially not for the large porosity systems. This point certainly deserves further study. More data, generated for more different k' or k'' values are needed to test other equations, like for example the moment equation [15].

Fig. 4a and b shows the A and C terms constants obtained from the fitting with Eq. (2). Knowing that the A-term is generally considered as a measure for the "goodness of packing" [23], it is interesting to note that there seems to be a constant shift between the A term constants for three degrees of heterogeneity, whereas the C term value remains near or less independent of both the porosity and the degree of heterogeneity.

Turning now to the flow resistance ϕ_0 of the considered packings, ϕ_0 obviously depends much more strongly on the bed porosity than on the packing heterogeneity (Fig. 4c). Looking at the exact values of the flow resistance, the packing heterogeneity, however, also has a significant and complex influence. For example, going from the uniform packing case to the short-scale randomness cases leads to an increase of ϕ_0 from 725 to 853 for the $\varepsilon = 0.4$ case. In the $\varepsilon = 0.6$-case, the flow resistance increase caused by the random distribution of the particles is already much smaller (going only from $\phi_0 = 168$ to 177), and in the $\varepsilon = 0.8$-case, the flow resistance in the random packing case is even slightly smaller than in the uniform packing case (respectively, $\phi_0 = 53$ to 50). The single general conclusion which can be drawn from these observations is that small porosity packings are much more prone to pore blocking. Comparing now the flow resistance of the short-scale randomness cases (cf. Fig. 1b) with the clustered packing cases (cf. Fig. 1c), it is found that the flow resistance in the latter case is always smaller, going from $\phi_0 = 853$ to 811 for $\varepsilon = 0.4$, from $\phi_0 = 177$ to 151 for $\varepsilon = 0.6$ and from $\phi_0 = 50$ to 41 for $\varepsilon = 0.8$. Since the flow domains in clustered packing

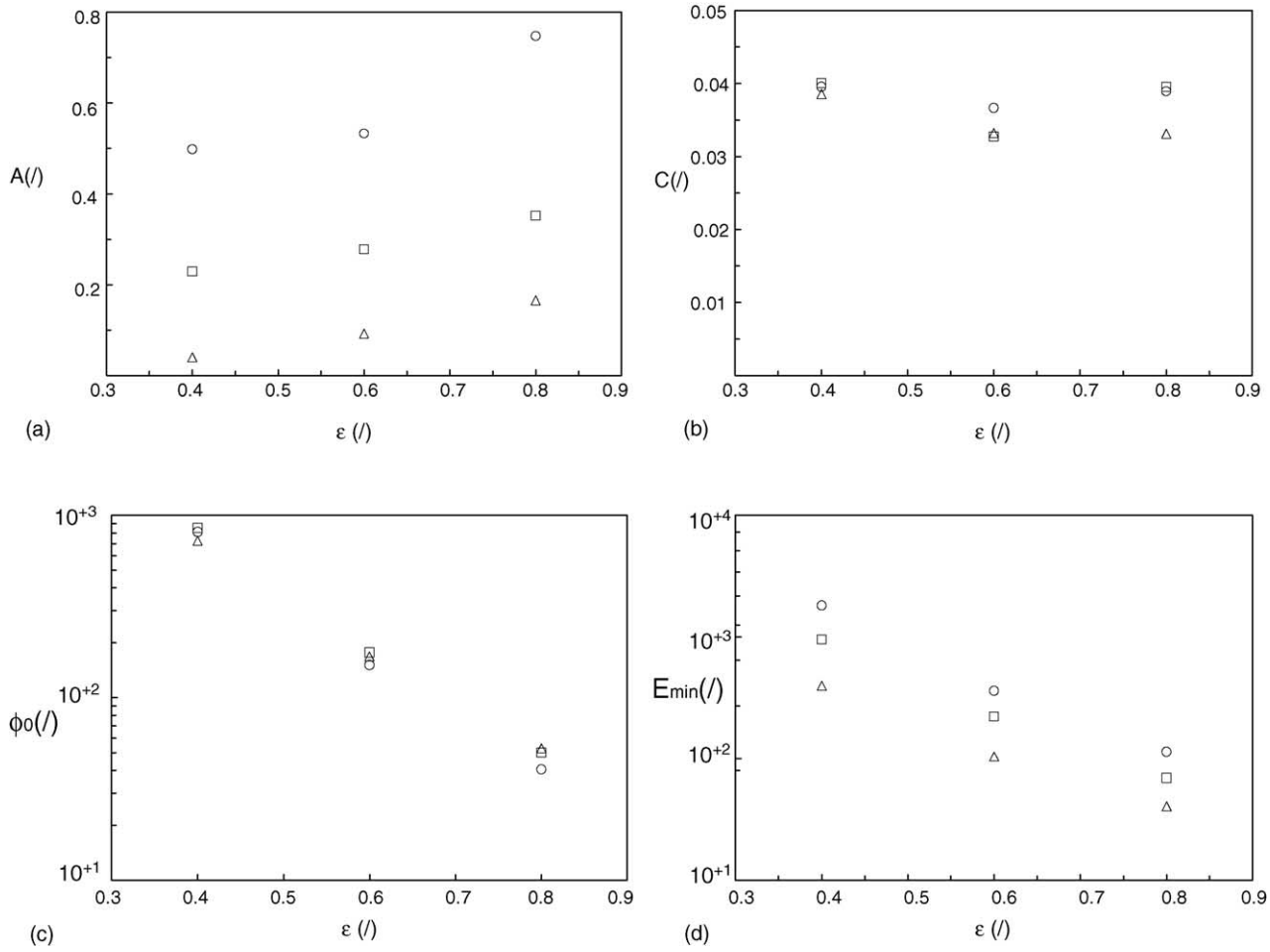

Fig. 4. Plot of the values of A, C, ϕ_0 and E_{min} as a function of ε and for the three different degrees of packing heterogeneity: (△) uniform array; (□) short-scale randomness packing; (◯) clustered packing. The A, C and ϕ_0 data relate to the d_{dom}-reduced case. Y-axis of (c) and (d) is plotted on a logarithmic scale.

cases have been obtained by starting from the geometries of short-scale randomness case and by bringing a number of selected particles more closer to each other, the observed flow resistance reduction indicates that the smaller flow resistance of the preferential flow paths is predominant over the larger flow resistance of the more densely packed cluster regions. This can be explained as follows. Since the porosity is kept constant between the three different heterogeneity cases, an increase of the packing heterogeneity inevitably implies that some of the flow-through pores will be smaller than in the uniform packing case, whilst others will be larger. If these larger pores are connected over a distance covering several particle diameters, they form preferential flow paths, which can be regarded upon as some kind of flow highways. Given that the flow rate in a given pore is proportional to the 3rd power of the pore size (fourth power in 3D), the major part of the flow will pass through these preferential flow paths, such that the advantage of the lower flow resistance in these wide pores will prevail over the disadvantage of the large flow resistance in the more dense regions. This reasoning can also be made in a more mathematical sound way, as is demonstrated in [25].

It should be noted that the above discussion does not necessarily has to hold for packed beds filled with particles with a very broad particle size distribution. In this case, there is a very large probability that the uniform particle size column and the disperse particle size column will have a different porosity, and it might very well be that this different porosity, either larger or smaller, has a larger impact than the difference in packing heterogeneity. Consider for example the case of a disperse particle mixture. In this case, the smaller particles may tend to fill up the larger pores, leading to an overall larger flow resistance as compared to the more uniform particle case. The intercalated smaller particles will, however, inevitably lead to a porosity decrease such that the uniform and the heterogeneous packing are no longer compared on the basis of the same porosity.

With the h_{min}-values from Fig. 2b and with the ϕ_0 values from Fig. 4c, it is straightforward to calculate the minimal separation impedance number $E_{min} = h^2\phi_0$, as defined by Knox [13]. Fig. 4d clearly shows that the separation impedance increases with increasing packing heterogeneity. The difference between the short-scale randomness data and the clustered packing data clearly shows that the advantage of the smaller flow resistance stemming from the presence of the large dominant preferential flow paths in the clustered packing case is more than outweighed by the much larger increase in minimal plate height. Whether or not this is a general rule which holds in every type of 3D-packings also requires further investigation.

4. Conclusions

Although the obtained data are for a series of 2D geometries, which strongly simplify the actual packing geometry of real LC columns, they provide a framework to explain many of the experimental observations in real packed and monolithic LC supports. The data also clearly illustrate the direct link between the details of the flow field and the band broadening in LC columns. Whereas this link has up to now always been discussed in a rather descriptive manner, the current simulations clearly show how the existence of radially distributed zones with a different velocity lie at the basis of the *A*-term band broadening (especially if these zones persist over a long axial distance), and that the radial extent of these zones serves as the main resistance to a radial re-equilibration between these zones.

Considering conditions wherein the diffusivity and the phase retention coefficient k' of the species are kept constant, it is found that the domain size reduced h_{min}-values are nearly independent of the external porosity and can hence be used as a measure for the degree of packing heterogeneity of real columns. With increasing packing heterogeneity, this domain size-reduced h_{min}-value increases from $h_{min} = 0.8$ for perfectly ordered supports, over $h_{min} = 1.1$ for disordered packings with a purely short-scale randomness and to $h_{min} = 1.5$ for disordered packings with larger scale heterogeneities. All these values are quasi-independent of the porosity. The $h_{min} = 1.5$ value furthermore corresponds quite nicely to the d_{dom}-reduced experimental plate height data for packed beds and large domain silica monoliths found in literature. The best possible $\varepsilon = 60\%$ monoliths are currently still 0.3 h units away from this minimum. For all porosities, the minimal d_{dom}-reduced plate height seems to be situated around $h = 0.8$, i.e., about two times smaller than the best possible real column systems. This difference points at the large potential gain in separation performance which can be obtained if it would be possible to produce perfectly uniform packings. This remark was already made earlier by Knox [26], but the present study now provides a quantitative support for his argumentations.

Acknowledgements

The authors greatly acknowledge a research grant (FWO KNO 81/00) from the Fund for Scientific Research-Flanders (Belgium). P.G. is supported through a specialization grant from the Instituut voor Wetenschap en Technologie (IWT) of the Flanders Region (grant no. SB/11419). The authors also gratefully acknowledge stimulating discussions with Peter Schoenmakers and Sebastiaan Eeltink from the University of Amsterdam (The Netherlands).

References

[1] R.E. Majors, LC GC Eur. 16 (6a) (2003) 8.
[2] G. Rozing, LC GC Eur. 16 (6a) (2003) 14.
[3] S. Hjertén, L.J. Liao, R.J. Zhang, J. Chromatogr. 473 (1989) 273.
[4] L.J. Liao, S. Hjerten, J. Chromatogr. 457 (1988) 165.
[5] F. Svec, J.M. Frechet, Anal. Chem. 64 (1992) 820.

[6] H. Minakuchi, K. Nakanishi, N. Soga, N. Ishizuka, N. Tanaka, Anal. Chem. 68 (1996) 3498.
[7] N. Tanaka, H. Kobayashi, N. Ishizuka, H. Minakuchi, K. Nakanishi, K. Hosoya, T. Ikegami, J. Chromatogr. A 965 (2002) 35.
[8] M. Motokawa, H. Kobayashi, N. Ishizuka, H. Minakuchi, K. Nakanishi, H. Jinnai, K. Hosoya, T. Ikegami, N. Tanaka, J. Chromatogr. A 961 (2002) 53.
[9] F. Svec, LC GC Eur. 16 (6a) (2003) 24.
[10] N. Vervoort, P. Gzil, G.V. Baron, G. Desmet, Anal. Chem. 75 (2003) 843.
[11] M. Al-bokari, D. Cherrak, G. Guiochon, J. Chromatogr. A 975 (2002) 275.
[12] R.T. Kennedy, J.W. Jorgenson, Anal. Chem. 61 (1989) 1128.
[13] P.A. Bristow, J.H. Knox, Chromatographia 10 (1977) 279.
[14] J.C. Giddings, Dynamics of Chromatography, Part I, Marcel Dekker, New York, 1965.
[15] G. Guiochon, S.G. Shirazi, A.M. Katti, Fundamentals of Preparative and Nonlinear Chromatography, Academic Press, London, 1994.
[16] U. Tallarek, E. Bayer, G. Guiochon, J. Am. Chem. Soc. 120 (1998) 1494.
[17] E. Grushka, L.R. Snyder, J.H. Knox, J. Chromatogr. Sci. 13 (1975) 25.
[18] J.H. Knox, Ann. Rev. Phys. Chem. 24 (1973) 29.
[19] J.J. Meyers, A.I. Liapis, J. Chromatogr. A 827 (1998) 197.
[20] P. Gzil, N. Vervoort, G.V. Baron, G. Desmet, Anal. Chem. 75 (2003) 6244.
[21] P. Gzil, J. De Smet, N. Vervoort, H. Verelst, G.V. Baron, G. Desmet, J. Chromatogr. A 1030 (2004) 53.
[22] J. De Smet, P. Gzil, N. Vervoort, H. Verelst, G.V. Baron, G. Desmet, Anal. Chem. 76 (2004) 3716.
[23] J.H. Knox, J. Chromatogr. A 831 (1999) 3.
[24] H. Minakuchi, K. Nakanishi, N. Soga, N. Ishizuka, N. Tanaka, J. Chromatogr. A 797 (1998) 121.
[25] P. Gzil, N. Vervoort, G.V. Baron, G. Desmet, J. Sep. Sci. 27 (2004) 887.
[26] J.H. Knox, J. Chromatogr. A 960 (2002) 7.